THE UNIVERSITY *of* EDINBURGH

Edinburgh Research Explorer

High Absorption Coefficient Cyclopentadithiophene Donor-Free Dyes for Liquid and Solid-State Dye-Sensitized Solar Cells

OPEN ACCESS

High Absorption Coefficient Cyclopentadithiophene Donor-free Dyes For Liquid and Solid-state dye-sensitized Solar Cells

Yue Hu,[a,d] Antonio Abate,[b,c] Yiming Cao,[b] Aruna Ivaturi,[a] Shaik Mohammed Zakeeruddin,[b] Michael Grätzel[b] and Neil Robertson*[a]*

[a] School of Chemistry, University of Edinburgh, King's Buildings, Edinburgh, EH9 3FJ, UK.

[b] Laboratory of Photonics and Interfaces, Swiss Federal Institute of Technology (EPFL), Station 6, Lausanne, Switzerland. [c] Adolphe Merkle Institute, Fribourg, Switzerland. [d] Wuhan National Laboratory for Optoelectronics (WNLO), Huazhong University of Science and Technology (HUST), 1037 Luoyu Road, Wuhan, Hubei Province, P.R.China 430074

Abstract

We report a series of 'donor-free' dyes, featuring moieties of oligo(4,4-dihexyl-4H-cyclopenta[1,2-b:5,4-b']dithiophene) (CPDT) functionalized with cyanoacrylic end groups for mesoscopic titania solar cells based on I^-/I_3^- or Co(II)/Co(III) redox couple and spiro-OMeTAD hole transporter. These were compared with similar cells using an oligo(3-hexylthiophene) dye (5T) which we have reported before. Extending the CPDT moiety of the dye molecules from one to three (denoted as CPDT-1, CPDT-2 and CPDT-3) widens the photoresponse overlap with the solar spectrum, increases the molar absorption coefficient up to 75000 $M^{-1}cm^{-1}$ and improves the short-circuit current (J_{SC}), open-circuit voltage (V_{OC}) and power conversion efficiency (PCE) for all types of DSSCs. Among these sensitisers, CPDT-3 shows the highest PCE of 6.7%, 7.3% and 3.9% with I^-/I_3^-, Co(II)/Co(III) redox couple and spiro-OMeTAD hole transporter, respectively, compared with 7.6%, 9.0% and 4.0% for 5T. Benefiting from the high absorption of CPDT-3, we demonstrate 900 nm-thick mesoporous TiO_2 film with remarkable J_{SC} of 10.9 mA cm^{-2} in solid-state DSCs.

Introduction

Over past two decades dye-sensitised solar cells (DSSC) have attracted enormous attention for particular applications.[1] DSSCs offer light-weight, coloured, flexible photovoltaic devices, free from toxic and scarce elements with record certified efficiency of 11.4%[2] and uncertified efficiency of 14.3%[3] under standard reporting conditions. One of the key components in a DSSC is the sensitiser, which controls light harvesting and charge separation. In recent years, metal-free organic dyes have been intensively studied due to their high absorption, flexible molecular tailoring and potentially low-cost synthesis, although the latter is mostly not true for high-efficiency dyes. Most organic dyes follow the same design strategy combining a donor head group, conjugated spacer and acceptor group which binds to the TiO_2; so-called D-π-A dyes.[4] Only in a very restricted number of cases, different structures have been reported.[5] In our work, Abate[6] et al reported the first example of a "donor-free" dye, 5T, which enhanced the performance of solid-state DSSCs compared with the D-π-A equivalent, MK2. Encouraged by this finding and from the facile synthesis of donor free dye molecules, we and others have also demonstrated high efficiency liquid electrolyte solar cells prepared with donor-free oligothiophene dyes.[7-8]

In these previous studies however, oligothiopehe dyes showed limited light harvesting with λ_{max} typically around 450 nm. In this study, we have therefore designed new donor-free dyes prepared with 4H-cyclopenta[2,1-b:3,4-b']dithiophene (CPDT) moieties to enhance the light absorption compared to donor free dyes prepared with oligothiophenes segments. CPDT units have been used for constructing the π-conjugated skeleton of organic sensitisers in many cases because of their co-planarity and strong electron donating capability.[9] Compared to two thiophene units as π-bridge, the fused CPDT π-group both red-shifts the visible light absorption maximum of the sensitiser and increases its molar extinction coefficient.[10-12] In addition, the easy introduction of

long alkyl chains on the bridging carbon atoms of CPDT can efficiently decrease the intermolecular interactions, which typically retards the electron recombination and thus improves V_{OC}.[13-15] Based on this idea, in this study a series of 'donor-free' sensitisers oligo(4,4-dihexyl-4H-cyclopenta[1,2-b:5,4-b']dithiophene) functionalized with cyanoacrylic end groups (CPDT-1, CPDT-2 and CPDT-3) were designed and synthesised easily using cross-coupling. Their optical and electronic properties were characterised through spectroscopic, electrochemical and computational techniques, showing versatile colour-tuning, and outstanding absorption coefficients up to 75000 $M^{-1}cm^{-1}$. They were used as effective sensitisers for mesoscopic titania solar cells with I^-/I_3^- or Co(II)/(III) redox couple and spiro-OMeTAD hole transporter. The solar cells were further studied by charge extraction experiments, intensity-modulated photovoltage spectroscopy (IMVS) and intensity-modulated photocurrent spectroscopy (IMPS). The performance of devices with the CPDT dyes were compared to the oligothiophene-based dyes to shed light on the working mechanisms of different π-groups used to prepared donor-free dyes.

Experimental Section

Synthetic procedure

Materials. All reagents were purchased from either Sigma-Aldrich or Alfa-Aesar and were used as received without further purification. 4H-cyclopenta[2,1-b:3,4-b']dithiophene was bought from Shanghai Qinghang Chemical Co. Ltd China. Synthesis of CPDT1, CPDT2, CPDT3 and precursors is described in the electronic supplementary information.

Methods

Instrumentation used for ^{1}H NMR, mass spectrometry, elemental analysis, electrochemistry and UV-Vis spectroscopy is as described in our earlier work. [7]

Electrochemical characterisation. Voltammetry measurements were carried out in anhydrous CH_2Cl_2 using 0.3 M [TBA][PF$_6$] electrolyte in a three-electrode system. The solution was purged with N_2 prior to measurement. The working electrode was a Pt disk. The reference electrode was Ag/AgCl and the counter electrode was a Pt rod. Cyclic voltammetry (CV) studies were carried out at scan rates of 0.1, 0.2, 0.4, 0.6, 0.8 and 1V/s. Square wave voltammetry (SWV) measurements used a scan rate of 40 mV/s with a step potential of 4 mV, amplitude of 25 mV and frequency of 15 Hz. Potentials are quoted against NHE for which ferrocene/ferrocenium was observed at 0.63 V.

Optical characterisation. All samples were measured in a 1 cm cell at room temperature with dichloromethane as a solvent. Concentration of 2×10^{-5} M was used for UV/Visible. A Beer-Lambert plot showed a linear response confirming no aggregation at this concentration. A concentration of 5×10^{-6} M was used for photoluminescence.

Computational details. The molecular structures were optimised in vacuum, using a starting geometry entered into Avogadro.[16] Then the structure was optimised in CH_2Cl_2, starting from the optimised structure from vacuum. Calculations were carried out with Gaussian 09[17] using the hybrid B3LYP functional)[18] and the 6-31G(d) basis set. Time-dependent DFT calculations (TD-DFT) were carried out using Gaussian 09 with a CH_2Cl_2 polarisable-continuum model (PCM)[19] using the CAM-B3LYP functional. The 20 lowest singlet electronic transitions were calculated and processed with the GaussSum software package. [20]

Solar cell fabrication. The liquid solar cells were made according to literature, [6] and full details are available in the ESI. Cells using I$^-$/I$_3^-$ electrolyte were based on 12 μm mesoporous layer + 6 μm scattering layer TiO_2 and the electrolyte 1M BMII, 0.05M GuNCS, 0.03M I$_2$, 0.05M LiI and 0.25M tBP in acetonitrile (4.25ml) and valeronitrile (0.75ml). Cells using Co electrolyte were

based on 6 μm of mesoporous layer + 4 μm scattering layer TiO_2 and the electrolyte 0.25M $[Co(bpy)_3(B(CN)_4)_2]$, 0.06M $[(Co(bpy)_3(B(CN)_4)_3)$, 0.1M LiTFSI and 0.5M tBP. The solid-state solar cells used a compact layer of TiO_2, 0.9 μm mesoporous TiO_2 and spiro-MeOTAD doped with 14 Li-TFSI, 112 mM TBP and 2.1 mM FK209. Finally, 80nm of gold was thermally evaporated on top of the device under high vacuum. The J-V measurements of I^-/I_3^- cells at 100 mWcm^{-2} used a light mask to fix the illuminated active area to 0.126 cm^2. J-V measurements of Co^{2+}/Co^{3+} cells and solid-state cells used a non-reflective metal mask of 0.16 cm^2. IPCE spectra were recorded under a constant white light bias of approximately 5mWcm^{-2} and excitation beam from a 300W Xenon lamp focused through a monochromator and chopped at approximately 2 Hz. IMPS, IMVS and charge extraction measurements were performed using a 625 nm LED driver at different light intensities and a Metrohm PGSTAT302N Autolab.

Results and Discussion

Synthesis

   The synthetic route of the oligo-CPDT series is shown in Scheme 1. Two hexyl chains were first introduced on the CPDT unit to attenuate the interfacial recombination, followed by palladium catalysed Stille coupling reactions and then Knoevenagel condensation to give CPDT-1, CPDT-2 and CPDT-3. CPDT-1 was obtained as an isomeric mixture with ratio 77:23 between trans- and cis- cyanoacrylic acid, as confirmed by ^{1}H NMR (Figure S1) and further separation was not possible by conventional purification techniques. This isomerization of the cyanoacrylic acid acceptor group has also been reported by Zietz, et al [21] using a simple D-π-A type dye where the donor triarylamine was connected with the cyanoacrylic acid acceptor via a double bond π-bridge.

However, no isomerization was observed for larger molecules, and in our case, CPDT-2 and CPDT-3 were found to be pure-trans by ^{1}H NMR (Figure S2 and Figure S3).
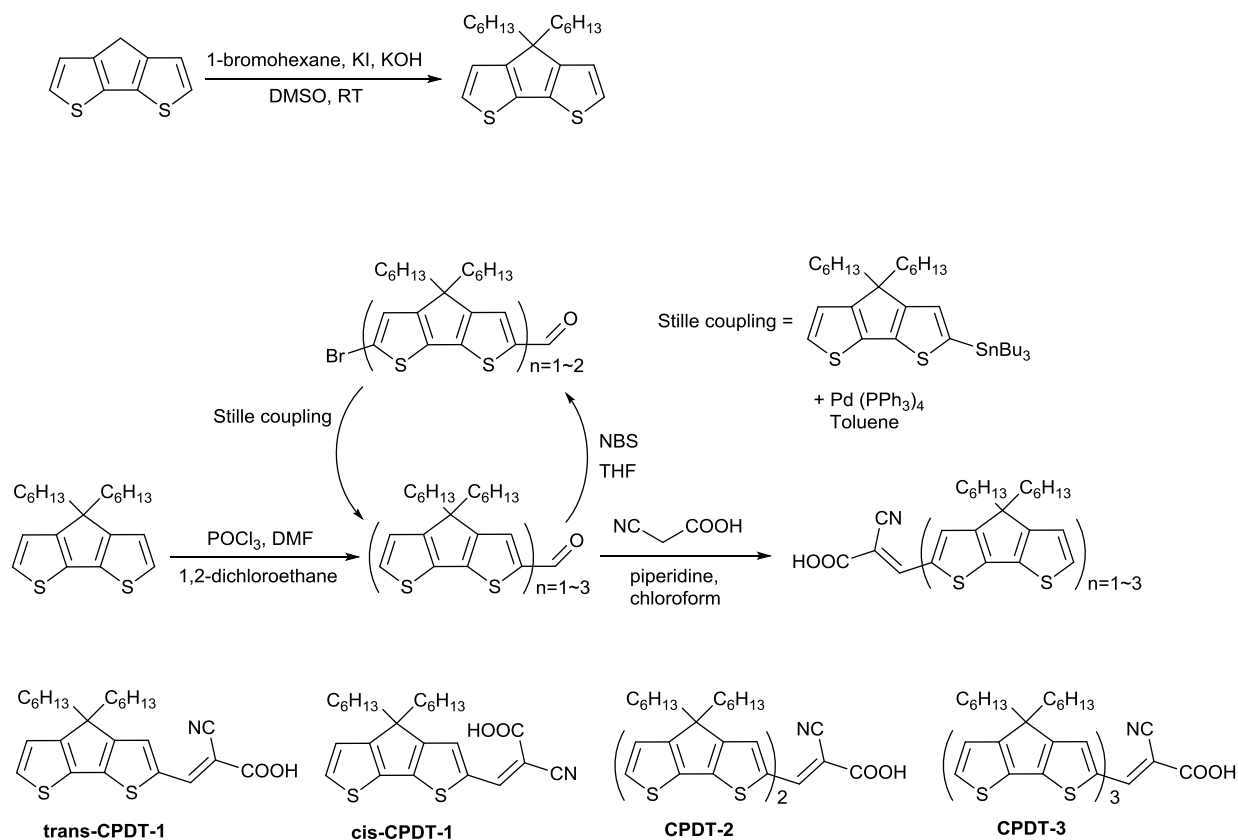
Scheme 1. Synthesis of CPDT series and their structures

Optical properties

Optical properties of the CPDT series were studied in dichloromethane solution (Figure 1) with data summarized in Table 1. A Beer-Lambert plot showed a linear response confirming no aggregation at this concentration. The addition of each CPDT unit led to an expected red shift in the UV-vis spectrum and an increase in the extinction coefficient, as shown in Figure 1. This is the result of the extra conjugation and electron delocalisation within the CPDT backbone, which reduces the molecular HOMO-LUMO gap. Although these oligo-CPDT dyes were engineered

with hexyl chains in order to reduce the tendency towards aggregation, the difference between the absorption spectra in solution and on film revealed that the aggregation cannot be suppressed fully with hexyl chains. The maximum absorption peaks of CPDT-2, CPDT-3 and 5T in dye-bath solution (0.2mM in 3:7 mixture of chloroform and ethanol) and on 0.9 μm film are also shown in Table 1 and the spectra are shown in Supporting Information (Figure S4 and Figure S5). In the case of 5T, a bathochromic shift was observed when the dye was bound to TiO_2, indicating the formation of J-aggregation. On the contrary, hypsochromic shifts were seen in the case of CPDT-2 and CPDT-3, indicating the formation of H-aggregation.[22]
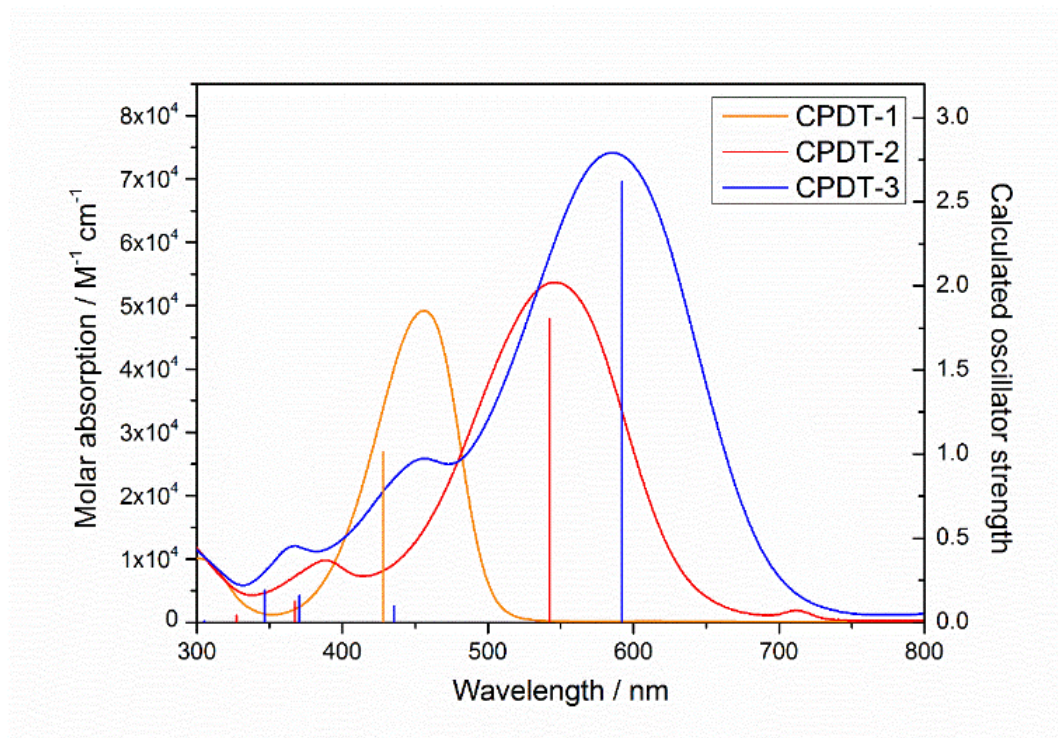

Figure 1. UV-vis absorption spectra of CPDT-1~3 in DCM with calculated electronic transitions represented as vertical lines.

Table 1. Photophysical and electrochemical properties of the CPDT series and 5T for comparison.

Dye	λ_{max}^a / nm (ε, $10^4 M^{-1} cm^{-1}$)	λ_{max}^b / nm	λ_{max}^c / nm	E_{ox}^d vs NHE / V	E_{red}^d vs NHE / V
5T	478 (3.9)	430	446	1.08	-1.29
CPDT-1	456 (4.9)	-	-	1.46	-1.54
CPDT-2	546 (5.4)	494	482	0.89	-1.48
CPDT-3	585 (7.4)	530	511	0.71	-1.44

[a] Absorption maximum of 10^{-5} M of dye molecules in dichloromethane. [b] Absorption maximum of 0.2 mM dye molecules in 3:7 mixture of chloroform and ethanol. [c] Absorption maximum of dye molecules on 0.9 µm-thick TiO_2 film. [d] Potential was measured in DCM with 0.3 M [TBA][PF$_6$] as electrolyte and calibrated with ferrocene/ferrocenium (Fc/Fc$^+$) as an internal reference and converted to NHE by addition of 0.63 V.

Electrochemical properties and DFT calculations

The redox potentials for CPDT-1~3 were obtained by cyclic voltammetry (CV) and square-wave voltammetry (SWV) (Figure 2) and are summarised in Table 1. Upon increasing CPDT core length, a clear trend in the oxidation potentials can be observed. The oxidation peaks gradually shifted to less positive potentials and the electrochemical gap between the first oxidation and first reduction potentials was reduced. The first oxidation process for CPDT-1 (Figure S6) is irreversible on the electrochemical time scale (0.1s to 1s). On the other hand, the first oxidation processes for CPDT-2 and CPDT-3 (Figure S7 and Figure S8) are reversible, although the first two oxidation processes are too close to be studied separately by cyclic voltammetry. For the reduction processes, a slight shift to less negative potential can be observed upon adding CPDT units. The shift is much smaller than

in the oxidation as the reduction processes is mainly controlled by the cyanoacrylic moiety, which is only marginally affected by the length of the chain.
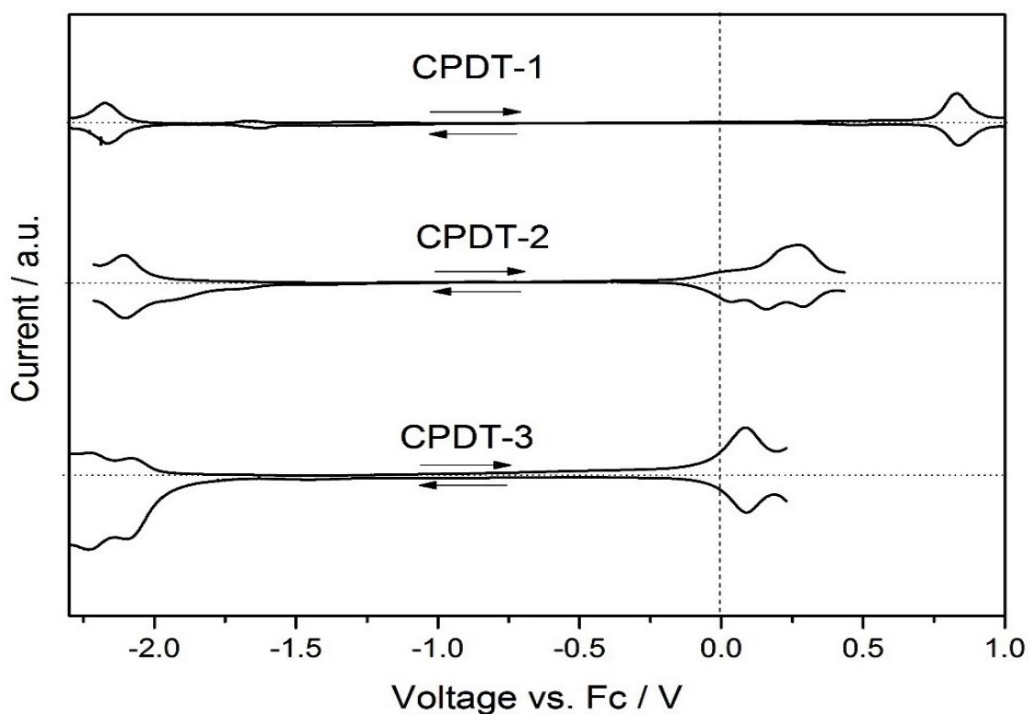

Figure 2. SWV of CPDT series recorded in DCM solution containing 0.3 M [TBA][BF$_4$] and referenced internally to ferrocene. Arrows indicate the direction of scan.

The energy level schemes for the Kohn-Sham orbitals of CPDT series, including selected Kohn-Sham orbitals and the HOMO-LUMO energy gap are shown in Figure 3. In all cases, the HOMO is mainly located on the CPDT core chain and the LUMO is located on the cyanoacrylic moiety, indicating good charge separation and appropriate charge directionality. The calculated HOMO and LUMO energy levels followed the same trend as that measured using electrochemistry.
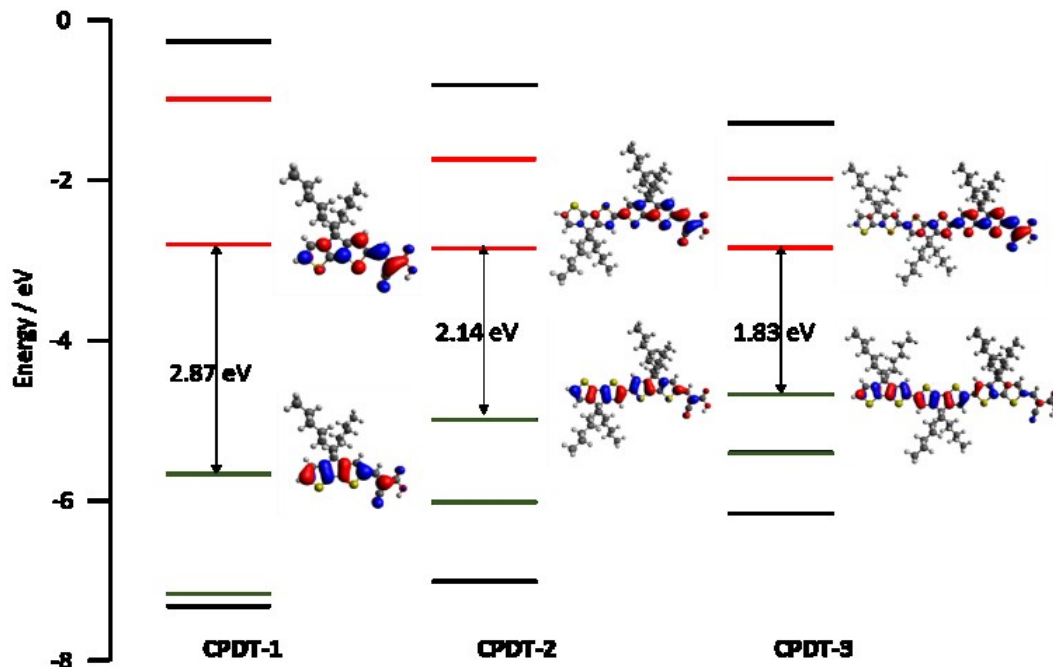
Figure 3. Molecular orbital distribution of HOMO (bottom) and LUMO (top) for CPDT series with their energy gap in DCM.

TD-DFT calculations were used to compare the theoretical and experimental electronic transitions through absorption spectroscopy. The calculations matched well with the experimental as shown in Figure 1. The lowest energy transitions of these dyes are dominated by HOMO→LUMO character. The maximum absorption band of CPDT-3 also has some contributions from HOMO-1→LUMO character. (Table S1) In addition, the calculations agree qualitatively well with experimental in molar extinction coefficient, whereby the oscillator strength (f) increased with the increasing CPDT chain length.

Photovoltaic performance of DSSCs

Due to the yellow colour of CPDT-1 which doesn't cover most of the solar spectrum, only CPDT-2 and CPDT-3 were further studied in devices, using 5T as comparison. They were examined in both liquid (I^-/I_3^- electrolyte or $[Co(bpy)_3]^{2+/3+}$ electrolyte) and solid-state DSSCs, for which the details of cell fabrication and data measurements are reported in the Experimental section. Three different thicknesses of TiO_2 were employed for these studies; 18 μm (12 μm mesoporous layer + 6 μm scattering layer) for I^-/I_3^- based cells, 10 μm (6 μm of mesoporous layer + 4 μm scattering layer) for $[Co(bpy)_3]^{2+/3+}$ based cells and 0.9 μm of mesoporous layer for spiro-based solid-state cells. Device performance parameters are shown in Table 2 with the corresponding J-V curves under light and dark condition reported in Supporting Information (Figure S9~S11). Upon addition of CPDT units, we can see an increase in J_{SC} and V_{OC}, which leads to an improvement of power conversion efficiency (PCE) moving from CPDT-2 to CPDT-3. Comparing with the DSSCs prepared with I^-/I_3^- electrolyte, the DSSCs with $[Co(bpy)_3]^{2+/3+}$ electrolyte showed a lower J_{SC} because of less dye adsorption from a thinner TiO_2 film. However, the V_{OC} of $[Co(bpy)_3]^{2+/3+}$ electrolyte based cells increased significantly, resulting in higher overall efficiencies. This increase of V_{OC} moving from I^-/I_3^- to $[Co(bpy)_3]^{2+/3+}$ electrolyte has been frequently observed[23] due to a lower loss-in-potential of the redox process.

Table 2. Photovoltaic parameters of solar cells using different redox couples and spiro-OMeTAD hole transporter under simulated AM 1.5G, 100mW cm^{-2} intensity illumination conditions.

Dye	Electrolyte	J_{SC} / mA cm^{-2}	V_{OC} / V	FF / %	η / %
5T	I[a]	17.2	0.62	72	7.6
CPDT-2	I[a]	11.2	0.53	67	4.0
CPDT-3	I[a]	18.0	0.57	66	6.7
5T	Co-bpy[b]	15.3	0.79	75	9.0
CPDT-2	Co-bpy[b]	9.7	0.67	76	4.9
CPDT-3	Co-bpy[b]	13.8	0.71	75	7.3
5T	Spiro[c]	6.5	0.85	67	4.0
CPDT-2	Spiro[c]	7.8	0.72	59	3.5
CPDT-3	Spiro[c]	10.9	0.73	47	3.9

[a] 1M BMII, 0.05M GuNCS, 0.03M I$_2$, 0.05M LiI and 0.25M tBP in acetonitrile (4.25ml) and valeronitrile (0.75ml). [b] 0.25M [Co(bpy)$_3$(B(CN)$_4$)$_2$], 0.06M [(Co(bpy)$_3$(B(CN)$_4$)$_3$), 0.1M LiTFSI and 0.5M tBP in acetonitrile. [c] 0.07 M spiro-OMeTAD, 0.112 M tBP, 0.014 M LiTFSI and 0.002 M FK209 in chlorobenzene.

The CPDT dyes show inferior performance to 5T in DSCs with liquid electrolytes or spiro-OMeTAD, mainly due to lower Voc. In cells using I$^-$/I$_3^-$ electrolyte, 5T showed a higher V_{OC} and FF than CPDT-3. In cells using [Co(bpy)$_3$]$^{2+/3+}$ electrolyte, 5T showed both a higher J_{SC} and a higher V_{OC} than CPDT-3, leading to a remarkable efficiency of 9%. The high efficiency of 5T we achieved in this study corroborates with the good results we previously reported for I$^-$/I$_3^-$ electrolyte[7] and questions the perceived necessity of a bulky donor group in sensitisers designed for Co-electrolyte based cells. [23] Although 5T shows inferior photon

harvesting capacity, the trade-off between light absorption length of sensitized TiO_2 film and charge diffusion length affords 5T a higher Jsc in DSSCs with 6+4 TiO_2 film in conjunction with cobalt complex redox couple. However, when the thickness of TiO_2 film reduces to 900 nm used in solid-state cells to facilitate spiro-OMeTAD infiltration and improve charge collection, the advantage of CPDT-2 and CPDT-3 with outstanding absorption coefficient affords higher Jsc (7.8 mA cm^{-2} and 10.9 mA cm^{-2}) than 5T (6.5 mA cm^{-2}). The extremely high J_{SC} of CPDT-3 on a TiO_2 film as thin as 0.9 um was not observed before with any other organic dye and is 30% higher than we found for Y123 (Figure S11), which has the record PCE in solid-state dye cells. However, the open-circuit voltage and fill factor of CPDT-2 (0.73V, 0.59) and CPDT-3 (0.72V, 0.47) could not compete with 5T (0.85V, 0.67).

Figure 4 exhibits the incident photon-to-current conversion efficiency (IPCE) spectra recorded on cells using $[Co(bpy)_3]^{2+/3+}$ electrolyte and solid-state cells. The J_{SC} data integrated from the IPCE spectra over all wavelengths against the solar spectrum are in good agreement with the experimental values. For cells using $[Co(bpy)_3]^{2+/3+}$ electrolyte, although CPDT-3 shows a broader IPCE spectrum to 800 nm, 5T has higher IPCE of ~65% from 400 nm to 600 nm than CPDT-3 (50%), thus resulting in a higher J_{SC}. For solid-state cells, CPDT-3 shows a broader and higher IPCE spectrum, which explains the exceptional J_{sc} we measure.
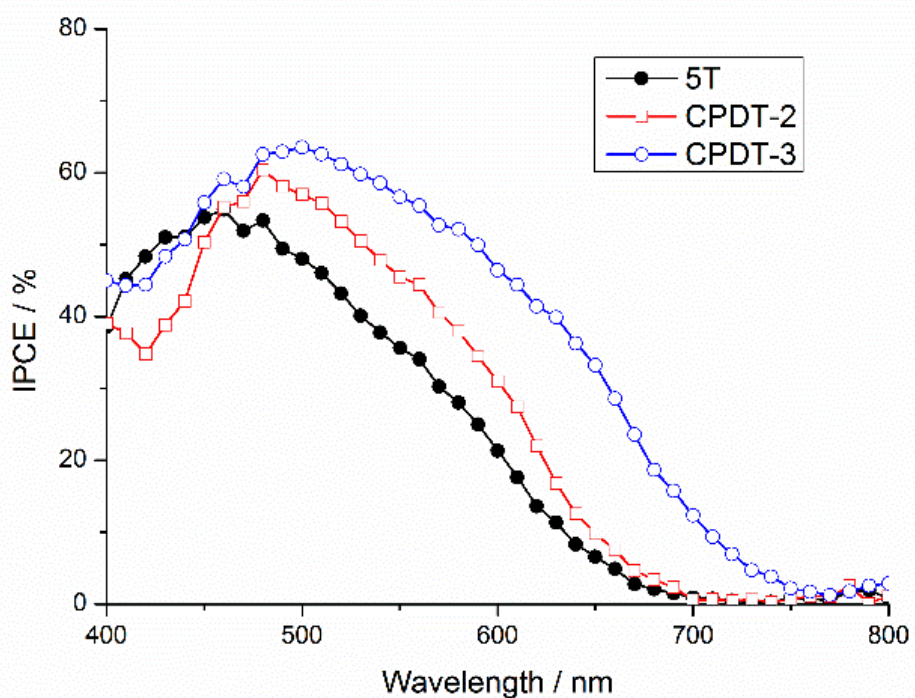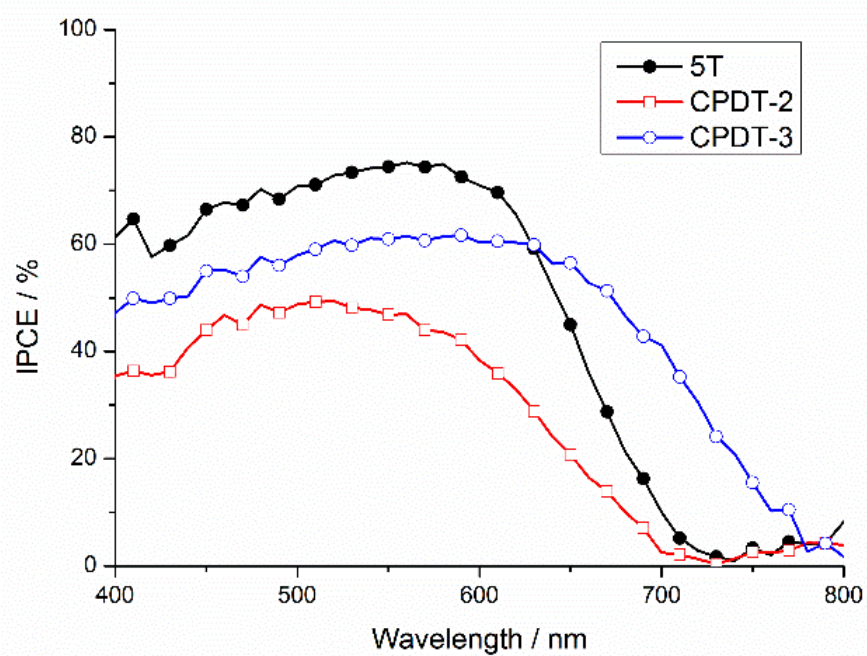
Figure 4. IPCE spectra for cells using $[Co(bpy)_3]^{2+/3+}$ electrolyte (upper) and spiro-OMeTAD (lower)

IMVS, IMPS and charge extraction

Overall, it was found that the V_{OC} of these dyes always follows the same trend no matter which electrolyte was used, namely 5T > CPDT-3 > CPDT-2. The open-circuit voltage is determined by the difference between the quasi-Fermi level of TiO_2 under illumination and the redox couple or HTM. This can be affected by 1) A shift of conduction band edge of TiO_2 caused by either dye attachment or additives like bis(trifluoromethane)sulfonimide lithium (Li-TFSI) and 4-tert-butylpyridine (tBP)[24]; 2) The number of electron trap states in the TiO_2 conduction band; 3) The charge recombination rate. In order to understand the predominant mechanism controlling the trend in V_{oc}, charge extraction (CE), intensity modulated photocurrent spectroscopy (IMPS) and intensity modulated photovoltage spectroscopy (IMPS) measurements were performed on the solid-state cells and $[Co(bpy)_3]^{2+/3+}$ electrolyte.

For solid-state cells, charge extraction measurements were first employed to find out the relationship between charge density and voltage. As shown in Figure 5 (upper), all the dyes have nearly identical charge density as a function of voltage. The charge extraction data were fitted to a mono-exponential, which enables comparison of the recombination lifetimes measured from IMVS at the same charge density, as reported in Figure 5 (lower). A significant difference in the recombination lifetime can be seen, ordering 5T > CPDT-2 > CPDT-3. This corresponds to the open-circuit voltage order of 5T > CPDT series we observed in devices. However, CPDT-3 shows a higher V_{OC} than CPDT-2 although the recombination lifetime is shorter. We suggest this may be due to the longer molecular length of CPDT-3, resulting in a larger dipole moment (Table S2) and thus a negative shift of the TiO_2 conduction band. It is clear that replacing the thiophene units of 5T with CPDT

units makes the recombination faster. CPDT-2 has the same number of alkyl chains as 5T and CPDT-3 has two more alkyl chains than 5T, so a simple relationship between alkyl chains and suppression of recombination can't explain what we observe.[25] One possibility is that 5T has a more twisted π-conjugated architecture than the CPDT dyes. Recently, the Li group designed a series of sensitisers with adjustment of the twist conformation through minor structural modifications and studied the effect of conjugation between the chromophore and anchoring group on the behaviour of solar cells. They found that sensitisers with better conjugation suffered from a severe back electron transfer although they showed better absorption properties.[26] In our case, computational calculations revealed that the dihedral angles between the thiophene units in 5T are from 20° to 35°, while those between the CPDT units in CPDT-2 and CPDT-3 are from 0° to 8° (Figure S12). The better conjugation of the CPDT dyes could lead to a problem of back electron transfer to the dye. In the case of solid-state DSSCs, another possibility is that the low regeneration driving force for CPDT-2 and CPDT-3 makes regeneration less competitive with recombination. Indeed, CPDT-2 (0.89V vs. NHE) and CPDT-3 (0.71V vs. NHE) are much easier to oxidise than 5T (1.02V vs. NHE). （Figure 6） Especially for CPDT-3, the oxidation potential in solution is even slightly less positive than spiro-OMeTAD.[27] Although energy levels may slightly change in the device, it is likely that an unfavourable energy offset can cause inefficient regeneration and hence a problem of charge recombination.[28] This problem would be solved if an easier to oxidise hole-transport material can be used instead of spiro-OMeTAD, but so far, no such highly-performing HTM has been developed.
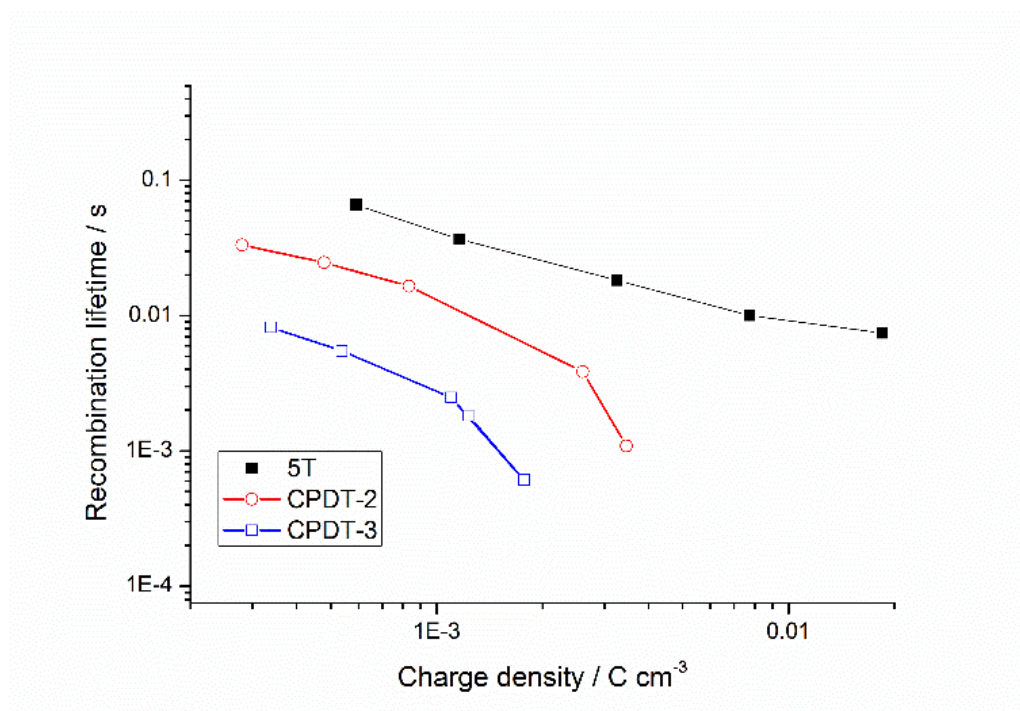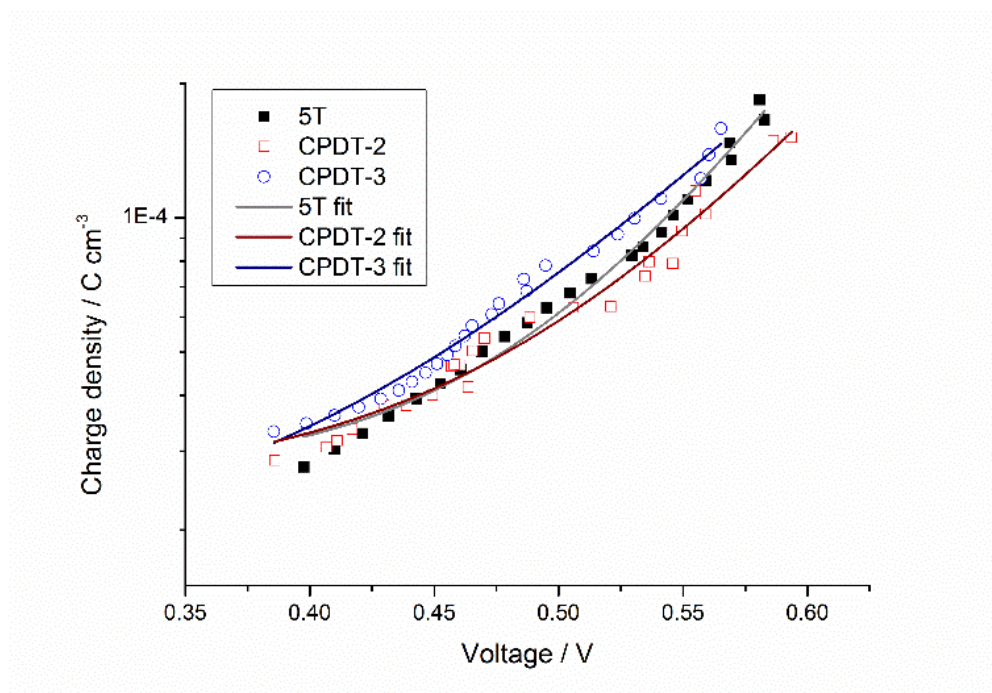
Figure 5 Charge extracted at a certain voltage for devices prepared with 5T and CPDT dyes using spiro-OMeTAD as hole transporter. Data are fitted to a monoexponential function. (upper) Recombination lifetime at open circuit conditions against charge density. (lower)
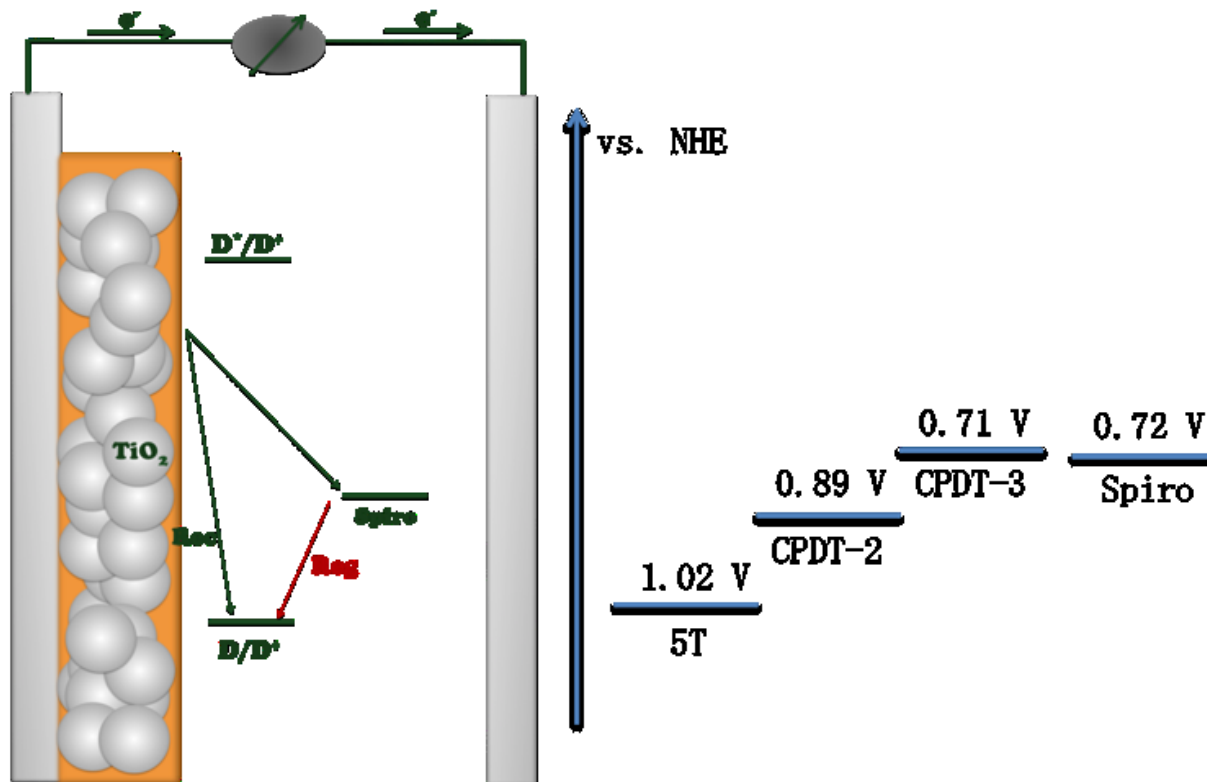
Figure 6 Energy level diagram of 5T, CPDT-2, CPDT-3 and spiro-OMeTAD (measured by electrochemistry).

For cells based on $[Co(bpy)_3]^{2+/3+}$ electrolyte, a qualitative image of the density of states (DOS) was extracted from the charge extraction experiment presented in Figure 7 (upper). Surprisingly, at the same open circuit voltage, CPDT-3 induces a significantly higher charge density in the device compared to the other dyes. This was not the case for the solid-state cells, in which all the dyes reported very similar charge density as a function of voltage (see Figure 5 upper). Therefore, when CPDT-3 is used with $[Co(bpy)_3]^{2+/3+}$ electrolyte a significant fraction of the photogenerated charge is accumulated in the device. Interestingly, the recombination lifetimes of the CPDT-3 devices are similar to the other dyes regardless of the fact that the charge density is more than one order of magnitude higher. (Figure 7 lower) This result was unexpected and points towards an unusual

influence of the different CPDT dyes on the characteristics of the TiO$_2$ which has no immediate explanation from the information presently available and requires further detailed investigation.
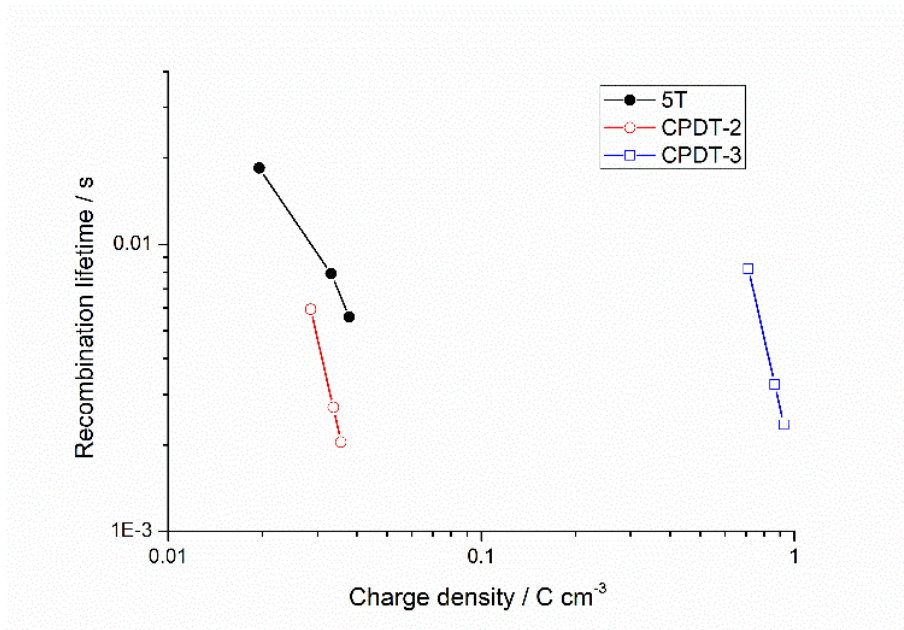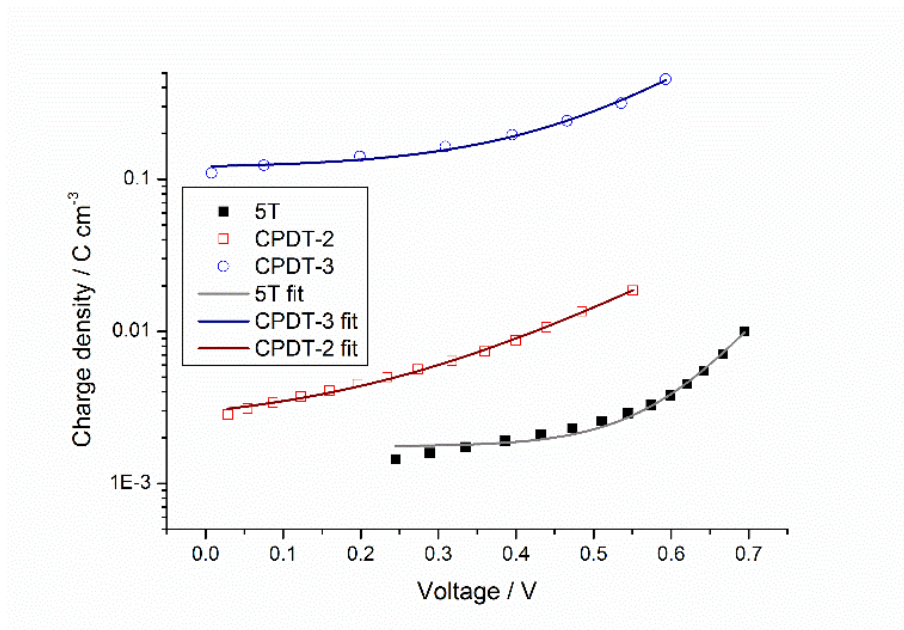
Figure 7. Charge extracted at a certain voltage for devices prepared with 5T and CPDT dyes using $[Co(bpy)_3]^{2+/3+}$ electrolyte. Data are fitted to a monoexponential function. (upper) Recombination lifetime at open circuit conditions against charge density. (lower)

Conclusion

A series of 'donor-free' dyes oligo(4,4-dihexyl-4H-cyclopenta[1,2-b:5,4-b']dithiophene) (denoted as CPDT-1, CPDT-2 and CPDT-3) functionalized with cyanoacrylic end groups was prepared by a simple synthesis using cross-coupling. The CPDT-2 and CPDT-3 dyes were used as effective sensitisers for mesoscopic titania solar cells with I^-/I_3^- or $[Co(bpy)_3]^{2+/3+}$ redox couple and spiro-OMeTAD hole transporter. The J_{SC}, V_{OC} and PCE increase upon addition of CPDT units in all types of DSSCs. As a result, CPDT-3 shows the highest efficiency among this series (6.7% for I^-/I_3^- based cells, 7.3% for $[Co(bpy)_3]^{2+/3+}$ based cells and 3.9% for solid-state cells). In solid-state dye-sensitised solar cells, CPDT-3 shows a remarkable J_{SC} of 10.9 mA cm^{-2} with only 900 nm mesoporous TiO$_2$ film due to the broad absorption over the solar spectrum and outstanding absorption coefficient of 75000 M^{-1}cm^{-1}. However, the CPDT dyes suffer from a low V_{OC} compared to the donor free oligo(3-hexylthiophene) dye (5T). By using charge extraction experiments, IMVS and IMPS, it was found that with spiro-OMeTAD the charge recombination across the TiO$_2$-dye-electrolyte interface is significantly higher in CPDT than 5T devices. We attributed this to the planar conformation of CPDT-3, which induces back electron transfer. Therefore, the high extinction coefficient and the broad absorption spectra make the CPDT unit an extremely promising basis for the further design of highly efficient donor-free dyes, but further optimization is necessary to address the recombination, such as inducing some

twist in the conformation of the π-system. Very interestingly, we found that when CPDT-3 is used with $[Co(bpy)_3]^{2+/3+}$ electrolyte the recombination is rather low despite the fact that the charge density is more than one order of magnitude higher than in 5T or CPDT-2 based devices. This result was unexpected and demonstrates that donor-free dyes may show new mechanistic features compared with standard designs and may open up new opportunities to design low-cost dyes for highly-efficient solar cells.

Supporting Information. The following files are available free of charge.

NMRs of the final products, UV-vis spectra, cyclic voltammetries of 5T, CPDT-2, CPDT-3, computational chemistry results, J-V curves (PDF)

Corresponding Author

* Neil Robertson, neil.robertson@ed.ac.uk, Tel: +44 131 6504755

* Antonio Abate, antonio.abate@epfl.ch, Tel: +41 21 69 33605

Author Contributions

The manuscript was written through contributions of all authors. All authors have given approval to the final version of the manuscript.

REFERENCES

1.   Yoon, S.; Tak, S.; Kim, J.; Jun, Y.; Kang, K.; Park, J., Application of Transparent Dye-Sensitized Solar Cells to Building Integrated Photovoltaic Systems. *Build. Environ* **2011**, *46*, 1899-1904.
2.   Han, L. Y.; Islam, A.; Chen, H.; Malapaka, C.; Chiranjeevi, B.; Zhang, S. F.; Yang, X. D.; Yanagida, M., High-Efficiency Dye-Sensitized Solar Cell with a Novel Co-Adsorbent. *Energ. Environ. Sci* **2012**, *5*, 6057-6060.
3.   Kakiage, K.; Aoyama, Y.; Yano, T.; Oya, K.; Fujisawab, J.; Hanaya, M., Highly-Efficient Dye-Sensitized Solar Cells with Collaborative Sensitization by Silyl-Anchor and Carboxy-Anchor Dyes. *Chem. Commun* **2015**, *51*, 15894-15897.
4.   Cappel, U. B.; Karlsson, M. H.; Pschirer, N. G.; Eickemeyer, F.; Schöneboom, J.; Erk, P.; Boschloo, G.; Hagfeldt, A., A Broadly Absorbing Perylene Dye for Solid-State Dye-Sensitized Solar Cells. *J. Phys. Chem. C* **2009**, *113*, 14595-14597.
5.   Hu, Y.; Robertson, N., Atypical Organic Dyes Used as Sensitizers for Efficient Dye-Sensitized Solar Cells. *Front. Optoelectron* **2016**, DOI: 10.1007/s12200-016-0568-5
6.   Abate, A.; Planells, M.; Hollman, D. J.; Stranks, S. D.; Petrozza, A.; Kandada, A. R. S.; Vaynzof, Y.; Pathak, S. K.; Robertson, N.; Snaith, H. J., An Organic "Donor-Free" Dye with Enhanced Open-Circuit Voltage in Solid-State Sensitized Solar Cells. *Adv. Energy. Mater* **2014**, *4*, 1400116
7.   Hu, Y.; Ivatuni, A.; Planells, M.; Boldrini, C.; Biroli, A. O.; Robertson, N., 'Donor-Free' Oligo(3-Hexylthiophene) Dyes for Efficient Dye-Sensitised Solar Cells. *J. Mater. Chem. A* **2015**.
8.   Demeter, D.; Roncali, J.; Jungsuttiwong, S.; Melchiorre, F.; Biagini, P.; Po, R., Linearly Π-Conjugated Oligothiophenes as Simple Metal-Free Sensitizers for Dye-Sensitized Solar Cells. *J. Mater. Chem. C* **2015**, *3*, 7756-7761.
9.   Chai, Q. P.; Li, W. Q.; Liu, J. C.; Geng, Z. Y.; Tian, H.; Zhu, W. H., Rational Molecular Engineering of Cyclopentadithiophene-Bridged D-a-Pi-a Sensitizers Combining High Photovoltaic Efficiency with Rapid Dye Adsorption. *Sci. Rep-Uk* **2015**, *5*.
10.   Li, R. Z.; Liu, J. Y.; Cai, N.; Zhang, M.; Wang, P., Synchronously Reduced Surface States, Charge Recombination, and Light Absorption Length for High-Performance Organic Dye-Sensitized Solar Cells. *J. Phys. Chem. B* **2010**, *114*, 4461-4464.
11.   Moon, S. J.; Yum, J. H.; Humphry-Baker, R.; Karlsson, K. M.; Hagberg, D. P.; Marinado, T.; Hagfeldt, A.; Sun, L. C.; Gratzel, M.; Nazeeruddin, M. K., Highly Efficient

Organic Sensitizers for Solid-State Dye-Sensitized Solar Cells. *J. Phys. Chem. C* **2009**, *113*, 16816-16820.

12.   Dualeh, A.; De Angelis, F.; Fantacci, S.; Moehl, T.; Yi, C. Y.; Kessler, F.; Baranoff, E.; Nazeeruddin, M. K.; Gratzel, M., Influence of Donor Groups of Organic D-Pi-a Dyes on Open-Circuit Voltage in Solid-State Dye-Sensitized Solar Cells. *J. Phys. Chem. C* **2012**, *116*, 1572-1578.

13.   Cui, Y.; Wu, Y. Z.; Lu, X. F.; Zhang, X.; Zhou, G.; Miapeh, F. B.; Zhu, W. H.; Wang, Z. S., Incorporating Benzotriazole Moiety to Construct D-a-Pi-a Organic Sensitizers for Solar Cells: Significant Enhancement of Open-Circuit Photovoltage with Long Alkyl Group. *Chem. Mater* **2011**, *23*, 4394-4401.

14.   Koumura, N.; Wang, Z. S.; Mori, S.; Miyashita, M.; Suzuki, E.; Hara, K., Alkyl-Functionalized Organic Dyes for Efficient Molecular Photovoltaics. *J. Am. Chem. Soc* **2006**, *128*, 14256-14257.

15.   Mosconi, E.; Yum, J. H.; Kessler, F.; Garcia, C. J. G.; Zuccaccia, C.; Cinti, A.; Nazeeruddin, M. K.; Gratzel, M.; De Angelis, F., Cobalt Electrolyte/Dye Interactions in Dye-Sensitized Solar Cells: A Combined Computational and Experimental Study. *J. Am. Chem. Soc* **2012**, *134*, 19438-19453.

16.   Hanwell, M. D.; Curtis, D. E.; Lonie, D. C.; Vandermeersch, T.; Zurek, E.; Hutchison, G. R., Avogadro: An Advanced Semantic Chemical Editor, Visualization, and Analysis Platform. *J. Cheminformatics* **2012**, *4*.

17.   Gaussian 09, R. A., M. J. Frisch, G. W. Trucks, H. B. Schlegel, G. E. Scuseria, M. A. Robb, J. R. Cheeseman, G. Scalmani, V. Barone, B. Mennucci, G. A. Petersson, *et al*, Gaussian, Inc., Wallingford CT, 2009.

18.   Becke, A. D., A New Mixing of Hartree-Fock and Local Density-Functional Theories. *J. Chem. Phys* **1993**, *98*, 1372-1377.

19.   Cossi, M.; Barone, V., Time-Dependent Density Functional Theory for Molecules in Liquid Solutions. *J. Chem. Phys* **2001**, *115*, 4708-4717.

20.   O'Boyle, N. M.; Tenderholt, A. L.; Langner, K. M., Cclib: A Library for Package-Independent Computational Chemistry Algorithms. *J. Comput. Chem* **2008**, *29*, 839-845.

21.   Zietz, B.; Gabrielsson, E.; Johansson, V.; El-Zohry, A. M.; Sun, L. C.; Kloo, L., Photoisomerization of the Cyanoacrylic Acid Acceptor Group - a Potential Problem for Organic Dyes in Solar Cells. *Phys. Chem. Chem. Phys* **2014**, *16*, 2251-2255.

22.   Guo, M.; Diao, P.; Ren, Y. H.; Meng, F. S.; Tian, H.; Cai, S. M., Photoelectrochemical Studies of Nanocrystalline Tio2 Co-Sensitized by Novel Cyanine Dyes. *Sol. Energ. Mat. Sol. C* **2005**, *88*, 23-35.

23.   Wu, K. L.; Hu, Y.; Chao, C. T.; Yang, Y. W.; Hsiao, T. Y.; Robertson, N.; Chi, Y., Dye Sensitized Solar Cells with Cobalt and Iodine-Based Electrolyte: The Role of Thiocyanate-Free Ruthenium Sensitizers. *J. Mater. Chem. A* **2014**, *2*, 19556-19565.

24.   Yang, J. B., et al., Influence of the Donor Size in D-Pi-a Organic Dyes for Dye-Sensitized Solar Cells. *J. Am. Chem. Soc* **2014**, *136*, 5722-5730.

25.   Barnes, P. R. F.; Miettunen, K.; Li, X. E.; Anderson, A. Y.; Bessho, T.; Gratzel, M.; O'Regan, B. C., Interpretation of Optoelectronic Transient and Charge Extraction Measurements in Dye-Sensitized Solar Cells. *Adv. Mater* **2013**, *25*, 1881-1922.

26.   Nguyen, W. H.; Bailie, C. D.; Burschka, J.; Moehl, T.; Gratzel, M.; McGehee, M. D.; Sellinger, A., Molecular Engineering of Organic Dyes for Improved Recombination Lifetime in Solid-State Dye-Sensitized Solar Cells. *Chem. Mater* **2013**, *25*, 1519-1525.

27.   Chai, Z. F., et al., Similar or Totally Different: The Adjustment of the Twist Conformation through Minor Structural Modification, and Dramatically Improved Performance for Dye-Sensitized Solar Cell. *Adv. Energy. Mater* **2015**, *5*.

28.   Moia, D.; Cappel, U. B.; Leijtens, T.; Li, X.; Telford, A. M.; Snaith, H. J.; O'Regan, B. C.; Nelson, J.; Barnes, P. R., The Role of Hole Transport between Dyes in Solid-State Dye-Sensitized Solar Cells. *J. Phys. Chem. C* **2015**, *119*, 18975-18985.